© 2018. Published by The Company of Biologists Ltd | Journal of Experimental Biology (2018) 221, jeb178160. doi:10.1242/jeb.178160

RESEARCH ARTICLE

Bluegill sunfish use high power outputs from axial muscles to generate powerful suction-feeding strikes

Ariel L. Camp*,‡, Thomas J. Roberts and Elizabeth L. Brainerd

ABSTRACT

Suction-feeding fish rapidly expand the mouth cavity to generate high-velocity fluid flows that accelerate food into the mouth. Such fast and forceful suction expansion poses a challenge, as muscle power is limited by muscle mass and the muscles in fish heads are relatively small. The largemouth bass powers expansion with its large body muscles, with negligible power produced by the head muscles (including the sternohyoideus). However, bluegill sunfish – with powerful strikes but different morphology and feeding behavior – may use a different balance of cranial and axial musculature to power feeding and different power outputs from these muscles. We estimated the power required for suction expansion in sunfish from measurements of intraoral pressure and rate of volume change, and measured muscle length and velocity. Unlike largemouth bass, the sternohyoideus did shorten to generate power, but it and other head muscles were too small to contribute more than 5–10% of peak expansion power in sunfish. We found no evidence of catapult-style power amplification. Instead, sunfish powered suction feeding by generating high power outputs (up to 438 W kg^{-1}) from their axial muscles. These muscles shortened across the cranial half of the body as in bass, but at faster speeds that may be nearer the optimum for power production. Sunfish were able to generate strikes of the same absolute power as bass, but with 30–40% of the axial muscle mass. Thus, species may use the body and head muscles differently to meet the requirements of suction feeding, depending on their morphology and behavior.

KEY WORDS: XROMM, Fluoromicrometry, Muscle work, Muscle power, Shortening velocity

INTRODUCTION

Fish can capture food underwater by creating high-velocity fluid flows that rapidly suck nearby food and water into the mouth. These suction flows are generated as a fish quickly expands its mouth cavity, increasing volume and decreasing pressure in this space so that water – and ideally prey – is accelerated inside (reviewed in Day et al., 2015). To suction feed successfully, ray-finned fishes (Actinopterygii) rely on a highly kinetic cranial skeleton that allows the mouth cavity to expand three-dimensionally (Alexander, 1967). Mouth cavity volume may be increased through elevation of the neurocranium (dorsal expansion), depression of the lower jaw and hyoid apparatus (ventral expansion), and abduction of the suspensorium and operculum (lateral expansion) (Liem, 1967, 1978; Van Wassenbergh et al., 2005, 2009a). Any combination of these expansion systems may be used during suction feeding, which contributes to prey capture in most of the over 30,000 species of ray-finned fishes (reviewed in Lauder, 1985; Wainwright et al., 2015; Westneat, 2006).

Expanding the mouth cavity during suction feeding requires not only a mobile skeleton, but also considerable muscle power and work. Mechanical power is the product of force and velocity or, in a fluid system like suction feeding, the product of the rate of volume change and the change in pressure (e.g. Marsh et al., 1992). The simultaneous rapid increase in volume and large decrease in pressure of the mouth cavity during suction expansion requires substantial power. However, vertebrate muscles can only generate a limited amount of power. The power produced by an actively shortening muscle depends on many factors, but its maximum capacity is ultimately limited by its mass: larger muscles generate more power than smaller muscles, all else being equal. Meeting the requirements of powerful feeding behaviors, therefore, may be particularly challenging, as the muscles of the head region are generally much less massive than those of the rest of the body.

Researchers have long recognized that head muscles are likely too small to generate all the power required for suction expansion (Aerts et al., 1987; Alexander, 1970; Elshoud-Oldenhave, 1979), and that additional power may come from the body muscles: the epaxials and hypaxials (Fig. 1A). The primary expansive muscles in the head region include three cranial muscles – levator arcus palatini, levator operculi and dilator opercula – and a hypobranchial muscle, the sternohyoideus (hereafter referred to together as ‘cranial’ muscles). All are oriented to generate lateral and ventral expansion (Fig. 1A), and are electrically active during suction expansion (reviewed in Grubich, 2001; Lauder, 1985; Westneat, 2006), although cranial muscle shortening has been measured in only a few instances (Camp et al., 2015; Carroll and Wainwright, 2006; Van Wassenbergh et al., 2007). The epaxial muscles are often considered part of the feeding apparatus as they are the only muscles that can elevate the neurocranium and are consistently active during suction feeding (Lauder, 1985). Hypaxial muscles are less well studied, but are generally active during feeding and can contribute to suction expansion by retracting the pectoral girdle, and in turn the hyoid apparatus (Camp and Brainerd, 2014; Van Wassenbergh et al., 2007). These massive, fast-fibered body muscles have the potential to generate substantial power, which can be directly applied to the feeding apparatus during suction expansion.

Suction expansion has been shown to be powered almost exclusively by the axial muscles in one fish species, the largemouth bass (Camp et al., 2015). Bass have a large mouth opening (gape) and volume, fusiform body, and rely on a combination of suction and forward acceleration, i.e. ‘ram’, to capture prey (Norton and Brainerd, 1993). In bass, large regions –

Dept. of Ecology and Evolutionary Biology, Brown University, Providence, RI 02912, USA.
*Present address: Dept. of Musculoskeletal Biology, Institute of Ageing and Chronic Disease, University of Liverpool, Liverpool L7 8TX, UK.

‡Author for correspondence (Ariel_Camp@liverpool.ac.uk)

A.L.C., 0000-0002-3355-4312; T.J.R., 0000-0002-6345-9324; E.L.B., 0000-0003-0375-8231

Received 7 February 2018; Accepted 13 April 2018

Journal of Experimental Biology (2018) 221, jeb178160. doi:10.1242/jeb.178160

List of abbreviations

ACS	anatomical coordinate system
CFD	computational fluid dynamics
CT	computed tomography
DO	dilator operculi
JCS	joint coordinate system
L_i	initial muscle length
L_0	optimum muscle length
LAP	levator arcus palatini
LO	levator operculi
SH	sternohyoideus
V_{opt}	optimal muscle shortening velocity for power production
XROMM	X-ray reconstruction of moving morphology

extending just over half the body – of the epaxials and hypaxials shortened during suction expansion (Camp and Brainerd, 2014). Despite shortening more slowly than the predicted optimum velocity for power production, this large mass of musculature was capable of generating far more than the total power required for even the most powerful strikes (Camp et al., 2015). In contrast, the four cranial muscles together could not have generated more than 5% of the power for most strikes, due to their small mass. None of these muscles except the levator operculi even shortened during peak expansion power; instead, they functioned to transmit axial muscle power and control mouth expansion kinematics.

However, it remains unknown how other fishes – particularly those with different feeding behaviors and/or morphology than largemouth bass – use the cranial and axial muscles to power suction expansion. Bluegill sunfish are another well-studied suction-feeding species that are closely related to largemouth bass (Near et al., 2004) but differ morphologically and in their feeding kinematics. Where bass rely on ram, large volume changes and modestly low pressures in the buccal cavity [up to 20 kPa below ambient (Carroll and Wainwright, 2006)] to capture prey, sunfish use primarily suction with relatively little ram (Norton and Brainerd, 1993), very low buccal pressures [35–50 kPa below ambient (Higham et al., 2006a; Lauder, 1980)] and small, moderately rapid volume changes (Higham et al., 2006b). These kinematics suggest that sunfish produce powerful strikes and, although it remains to be experimentally demonstrated, it is reasonable to expect that the axial muscles generate much of that power, as they do in bass. Not only do sunfish have different feeding kinematics but, compared with the fusiform bass, they also have shorter, deeper and more laterally compressed bodies and a smaller gape (Fig. 1B) (Smith et al., 2015; Werner, 1977).

These differences make bluegill sunfish an interesting model for examining how cranial and axial muscles are used to power strikes in species that are behaviorally and morphologically distinct from largemouth bass. Sunfish could use a different mass of musculature by recruiting a larger or smaller region of the axial muscles for active shortening and/or by generating positive power from more cranial muscles (including the sternohyoideus). They could also generate relatively more power per unit muscle than bass, for example, by shortening their muscles at a speed closer to the predicted optimum for power production (Carroll et al., 2009). Alternatively, sunfish may use elastic energy storage to amplify their muscle power: shortening muscles slowly before the strike to load energy into an elastic element, and then releasing it much more rapidly at a higher power. Such a 'biological catapult' style of power amplification is typified by muscle activation and shortening preceding skeletal motion, and has been hypothesized in a suction-feeding cichlid fish (Aerts et al., 1987) and demonstrated in the axial muscles of pipefish and seahorses (Van Wassenbergh et al., 2008, 2009b). Like bass, pipefish also rely almost exclusively on the axial muscles to power suction feeding but, in this species, epaxial and hypaxial muscle power is amplified by loading energy into the long tendons that connect these muscles to the feeding apparatus (Van Wassenbergh

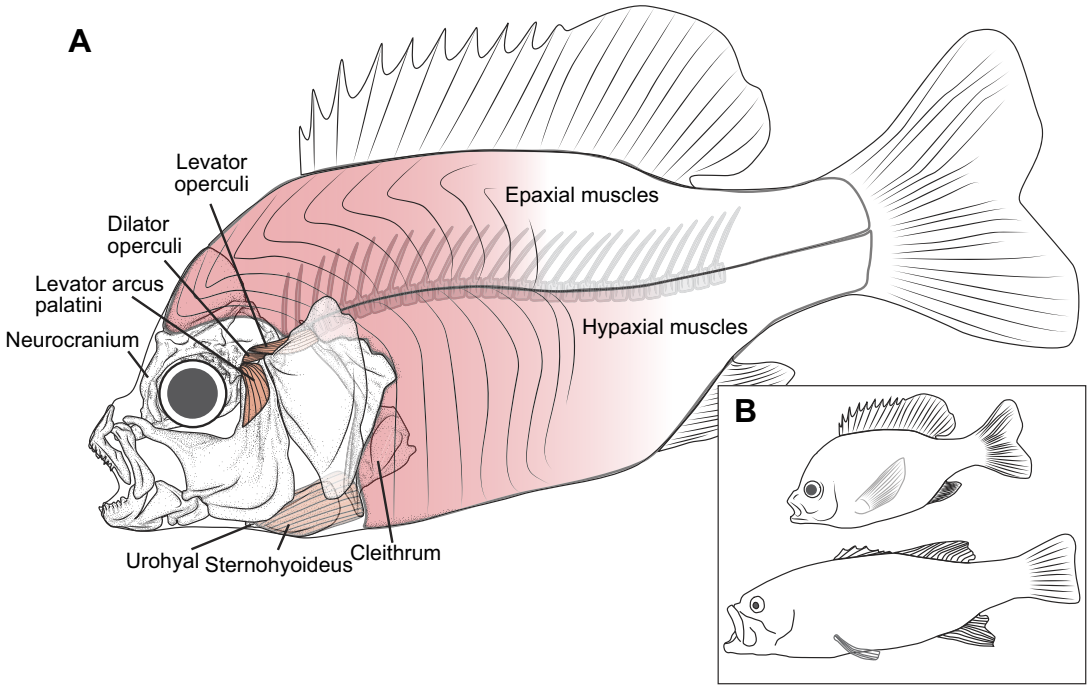

Fig. 1. Muscles of the feeding apparatus and the muscles of suction expansion in the bluegill sunfish. (A) The regions of the axial muscles that consistently shortened during suction feeding are colored solid red, with decreasing color intensity indicating generally decreasing shortening until ultimately regions without shortening are colorless (white). (B) Whole-body shape of bluegill sunfish (top) and largemouth bass (bottom).

et al., 2014, 2008). Power amplification cannot increase the total energy or work, so it still requires enough musculature to produce the necessary work of suction feeding. Our goal was to determine which of these strategies bluegill sunfish use to generate high-powered suction feeding: recruiting a large region of axial muscles for shortening, generating positive power from more cranial muscles, producing higher mass-specific power outputs from their cranial and/or axial muscles, and catapult-style power amplification of cranial and/or axial muscles.

To test these possibilities, we measured muscle shortening and expansion power to determine the roles of the cranial and axial muscles in powering suction feeding in bluegill sunfish. As the cranial and axial muscles are all known to be active during suction expansion in bluegill sunfish (Lauder and Lanyon, 1980; Lauder et al., 1986), we assumed that any muscle shortening was active and indicated power production. Muscle length changes throughout the epaxials and hypaxials were measured with fluoromicrometry, which uses biplanar X-ray video to measure the change in distance between radio-opaque, intramuscular markers (Camp et al., 2016). These X-ray videos were also combined with digital bone models to create accurate and precise skeletal animations of sunfish suction feeding with X-ray reconstruction of moving morphology (XROMM) (Brainerd et al., 2010). From the XROMM animations, we measured the skeletal kinematics of expansion, whole-muscle length changes of the four non-axial muscles and instantaneous volume changes of the buccal cavity [using a dynamic digital endocast (Camp et al., 2015)]. Buccal volume dynamics were combined with pressure measurements from an intraoral pressure probe to estimate the power and work required for suction expansion. Measurements of mass for each muscle were taken post-mortem and used to estimate mass-specific power and work production. These data allowed us to (1) estimate how powerful sunfish suction strikes are, (2) determine which cranial muscles and regions of the axial musculature shorten to generate power during suction feeding, and (3) test whether pre-shortening and elastic energy storage were used to amplify muscle power during suction expansion in bluegill sunfish.

MATERIALS AND METHODS

Two bluegill sunfish (*Lepomis macrochirus*, Rafinesque 1819) – bluegill 1 (standard length 170 mm, total mass 164 g) and bluegill 3 (standard length 167 mm and total mass 162 g) – were line-caught in Providence, RI, USA, under a scientific collecting permit from the Rhode Island Department of Environmental Management. All experimental procedures were approved by the Brown University Institutional Animal Care and Use Committee, RI, USA.

Each fish was anesthetized and surgically implanted with bone and muscle markers, and a cannula for a pressure probe. Implantation techniques followed previously reported methods (Camp and Brainerd, 2014; Camp et al., 2015) and are described briefly here. One to four radio-opaque markers (tantalum spheres, 0.5 mm diameter) were implanted in the neurocranium, urohyal and the left-side cleithrum, operculum, suspensorium, lower jaw (dentary and articular), maxilla and premaxilla (Fig. 1A). At least one marker was also implanted in the soft tissue of the esophagus to demarcate the back of the mouth cavity. Intramuscular markers (0.8 mm diameter) were implanted along the length of the epaxials (four markers) and hypaxials (three markers), within the muscle but close to the dorsal and ventral surfaces. An additional three markers implanted more deeply in the epaxials (Fig. 2A), together with three of the superficial epaxial markers, were used to define a dorsoventral body plane. Lastly, a cannula to house the pressure probe was implanted in the ethmo-frontal region following established methods (Norton and Brainerd, 1993). Fish were given a pre-operative analgesic (Butorphanol) and a postoperative antibiotic (enrofloxacin), and recovered fully within 3 days, with no signs of stress or difficulty caused by any of the implants.

Data recording

We filmed suction-feeding strikes from each fish with high-speed biplanar X-ray video and simultaneously recorded intraoral pressure (Camp and Brainerd, 2014; Camp et al., 2015). Fish were trained to feed on live goldfish prey in narrow (7×25.5×103.5 cm) tanks, as this minimized the volume of water the X-rays passed through and gave the highest quality images. Some individual bluegill were reluctant to feed on live prey, and non-elusive prey (pellets) yielded only low-motivation strikes, as judged by the magnitude of subambient pressure. We collected, trained, instrumented and recorded data from five individuals, but only two of these individuals, bluegills 1 and 3, fed on live prey. Therefore, we report data from just two individuals here because the focus of this study is high-performance strikes. Raw data from the other three bluegills feeding on pellets are potentially

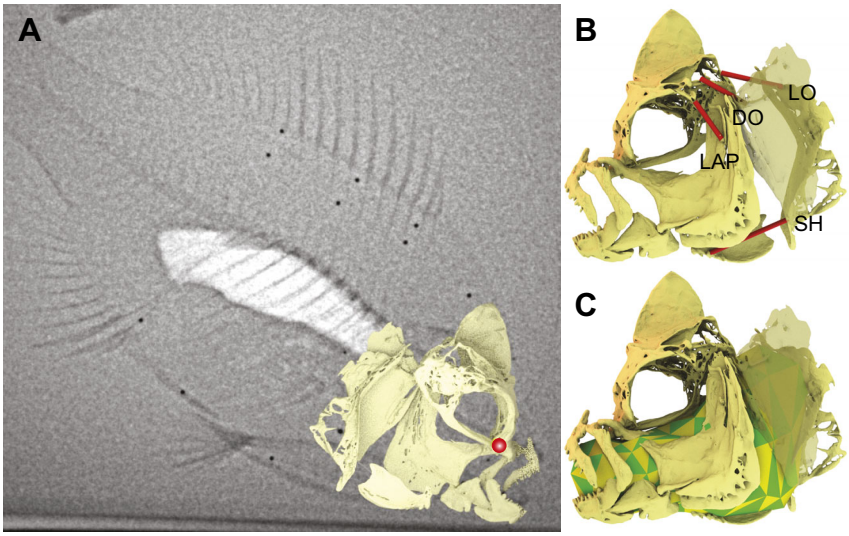

Fig. 2. Sample X-ray reconstruction of moving morphology (XROMM) animation and measurements of suction expansion. (A) Right medial-view X-ray image with animated bone models superimposed (neurocranium, urohyal and left-side bones only). Intramuscular markers for fluoromicrometry and the body plane are visible along the dorsal and ventral edge of the epaxial and hypaxial muscles, respectively. The location of the pressure transducer is indicated by the red sphere. (B,C) Left lateral view of animated bone models with (B) muscle length measurements (red lines) of the levator arcus palatini (LAP), dilator operculi (DO), levator operculi (LO) and sternohyoideus (SH) muscles, and (C) the dynamic digital endocast (green and yellow) used to measure volume.

available for further study (by communication with the authors). Metadata for all individuals, including number of strikes and food types, are viewable on XMA Portal (available at xmaportal.org, under study identifier BROWN48).

Approximately dorsoventral and lateral view X-ray videos were generated at 200 mA and 105 (dorsoventral view) or 65 (lateral view) kV with a custom-made biplanar system (Imaging Systems and Services, Painesville, OH, USA), and recorded at 500 frames s^{-1} with Phantom v10 high-speed cameras (Vision Research, Wayne, NJ, USA). Images were also recorded of standard grids and a calibration object – two sheets of acrylic embedded with 32 steel markers – to remove distortion introduced by the X-ray machines and calibrate the three-dimensional (3D) space imaged by both videos (Brainerd et al., 2010). Pressure was measured with a SPR-407 Mikro-tip pressure probe (Millar Instruments, Houston, TX, USA) inserted through the cannula, so it just protruded into the mouth cavity. Pressures were recorded at 1000 Hz with PowerLab and LabChart 7.2.2 (AD Instruments, Colorado Springs, CO, USA), and the probe was calibrated before each day of filming. A single trigger started both X-ray video and pressure recording, and daily synchronization tests measured the timing offset (if any) between the onset of pressure and video recordings. A total of 11 recorded strikes (six from bluegill 1, five from bluegill 3) were analyzed. The associated X-ray video, pressure and CT data (see below) are deposited and publicly available in the XMA Portal (available at xmaportal.org, under study identifier BROWN48).

Computed tomography (CT) scans were taken of each fish post-mortem with a Bruker Skyscan 1173 at a resolution of 0.13 mm $pixel^{-1}$ and a slice thickness of 0.13 mm. From these scans, polygonal mesh models of each bone and its markers were generated in Horos (v2.1.2; Horos Project; horosproject.org), and edited in GeoMagic 2013 (Research Triangle Park, NC, USA). The position of each bone marker was then measured relative to the 3D bone models in Maya 2016 (Autodesk, San Rafael, CA, USA) using custom scripts in the 'XROMM Maya Tools' package, available at https://bitbucket.org/xromm/xmalab.

XROMM

Skeletal kinematics were reconstructed with marker-based XROMM, using XMALab (Knörlein et al., 2016; software and instructions available at https://bitbucket.org/xromm/xmalab) and custom Maya scripts (available at https://bitbucket.org/xromm/xromm_mayatools). In XMALab, all markers were tracked in both X-ray videos to calculate their *xyz* coordinates with a tracking precision of 0.065 mm or better across all bones and both individuals, measured as the mean of the standard deviation of intraosseous marker distances (Brainerd et al., 2010). To improve contrast and ease of marker tracking, X-ray videos were first filtered with an unsharp mask in Adobe Photoshop (CC 2017, Adobe Systems). For bones with at least three markers, *xyz* coordinates were combined with marker positions relative to the 3D bone models to calculate rigid body transformations, which were filtered at 60 Hz low-pass Butterworth filter in XMALab and applied to the 3D bone models in Maya. The six epaxial markers of the body plane were treated as belonging to a single bone and used to calculate the rigid body transformations of a polygonal mesh plane (Camp and Brainerd, 2014). Bones with only one or two markers were animated in Maya with scientific rotoscoping: hand-aligning a bone model to match the images of that bone in both X-ray views (Gatesy et al., 2010). Both techniques were used to create a single XROMM animation of all marked bones during each suction-feeding strike (Fig. 2A, Movie 1).

Skeletal kinematics

From these XROMM animations, six-degree-of-freedom motions of the neurocranium, cleithrum and urohyal were measured relative to the body plane. Motions of each bone were measured with a joint coordinate system (JCS), which calculated the relative motion between two anatomical coordinate systems (ACSs) placed at a joint, one attached to the body plane and one attached to the bone (Camp and Brainerd, 2014). Each JCS measured skeletal kinematics as a set of translations along, and Euler angle rotations about, the *x*-, *y*- and *z*-axes, following the right-hand rule and a *zyx* order of rotation. For the neurocranium, the ACSs were placed at the craniovertebral joint, with the *z*-axis oriented mediolaterally, the *x*-axis rostrocaudally, and the *y*-axis orthogonal to both the *x*- and *z*-axes (Fig. 3A). Thus, the *x*-axis described rostrocaudal translation and long-axis rotation (roll), the *y*-axis described dorsoventral translation and mediolateral rotation (yaw), and the *z*-axis described transverse translation and rotation in the sagittal plane (cranial elevation/depression). The ACSs of the cleithrum and urohyal had the same orientation, but were placed at the rostrodorsal edge of the cleithrum (near the cleithrum–supracleithrum joint) and at the rostroventral protuberance of the urohyal, respectively (Fig. 3A).

Dynamic endocast and volume calculation

Volume changes of the buccal cavity were measured from the XROMM animations using a dynamic digital endocast, as described previously (Camp et al., 2015). Briefly, a polygonal mesh endocast was built to fill the left side of the mouth cavity, as defined by the animated bones (Fig. 2C), with the vertices of the polygonal endocast linked to skeletal landmarks so that the endocast deformed as the animated bones moved (Movie 2). The volume of this left-side endocast was calculated at each frame using a custom Maya script written by S. Gatesy, and doubled to give the volume of the whole buccal cavity, assuming bilateral symmetry.

Muscle length changes

Axial muscle length changes were measured from the biplanar X-ray videos using fluoromicrometry: measuring muscle length as the change in distance between intramuscular markers (Camp et al., 2016). Muscle markers were tracked and the *xyz* coordinates calculated in XMALab; all further calculations were done in MATLAB (R2015a; The Mathworks, Natick, MA, USA). Marker coordinates were filtered at 60 Hz (low-pass Butterworth filter), and the distance between each pair of markers (i.e. length change) calculated to determine which regions of the epaxial and hypaxial muscles consistently shortened during suction feeding. The rostralmost region of each muscle was defined as the distance between the rostralmost muscle marker and a bone marker at the muscle attachment site on the neurocranium or cleithrum. Muscle shortening was measured for every region, and all regions that consistently shortened were included in the whole-muscle length of each axial muscle (Fig. S1). Based on this, whole-muscle length of the epaxials was the distance from the neurocranium to the caudal edge of the first (spiny) dorsal fin (shaded region in Fig. 1A). Whole-muscle length of the hypaxial muscles extended from the ventral tip of the cleithrum to the rostral edge of the anal fin (shaded region in Fig. 1A). Note that these 'whole-muscle' lengths only represent shortening across the superficial regions of the axial muscles measured by fluoromicrometry. They may not necessarily be representative of fiber length changes outside of the region of measurement. Cranial muscle lengths were measured from the XROMM animations by calculating the distance between each

Journal of Experimental Biology (2018) 221, jeb178160. doi:10.1242/jeb.178160

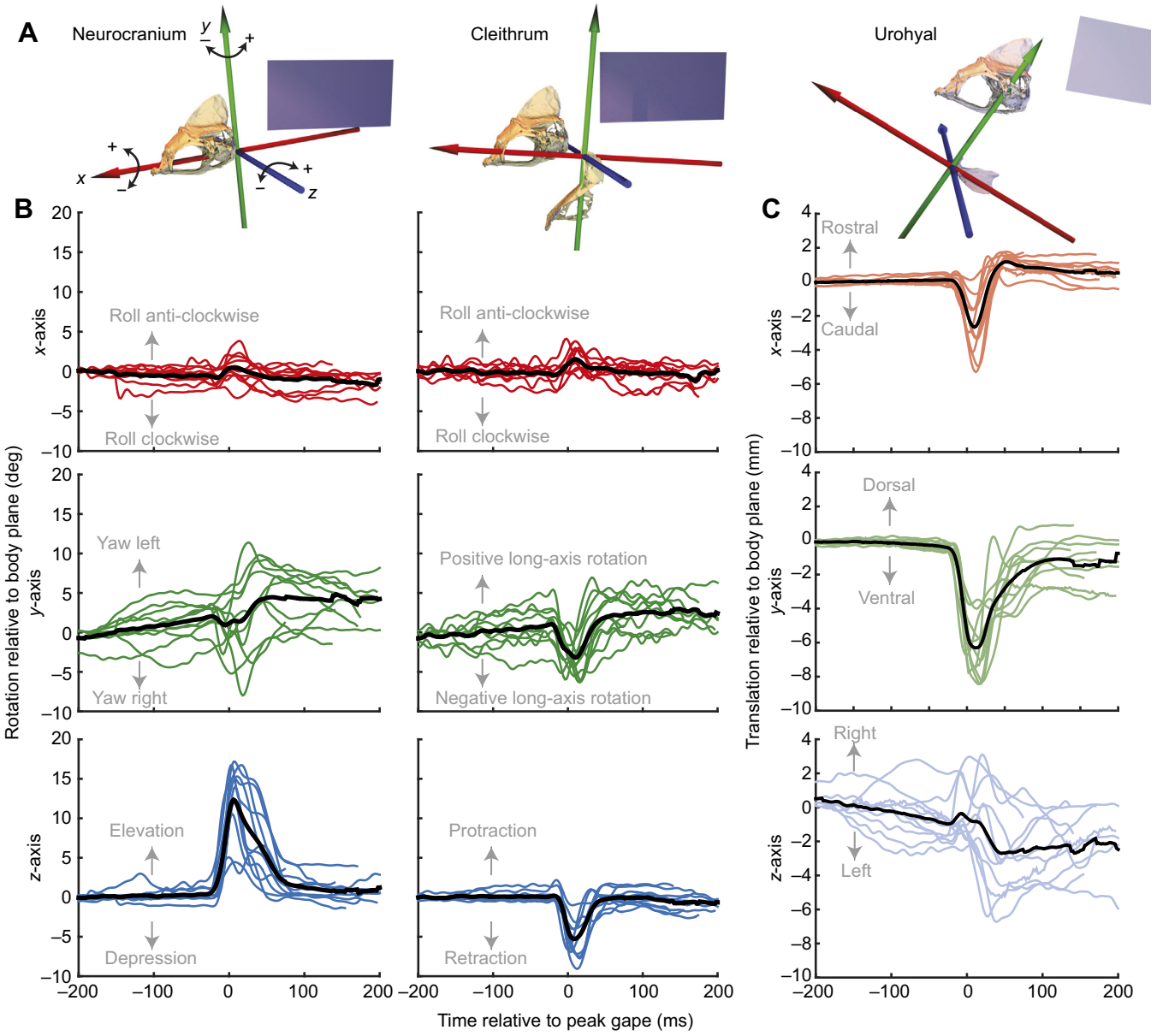

Fig. 3. Rotations of the neurocranium and cleithrum, and translations of the urohyal, relative to the body plane. (A) For each bone, rotations were measured about each axis of the joint coordinate systems. Euler angles were calculated with a *zyx* rotation order, with polarity determined by the right-hand rule with thumb pointed toward the arrowhead for each axis. Bone models are shown along with the body plane (blue rectangle). (B,C) Rotations (B) or translations (C) are shown from each strike (colored lines), as well as the mean rotation or translation (black lines) at each time step. Clockwise roll of the neurocranium and cleithrum are defined from a frontal view, and negative long-axis rotation of the cleithrum is clockwise in dorsal view. Means are calculated across both individuals and all strikes (*N*=11 strikes).

muscle's bony attachment sites (Camp et al., 2015). For each muscle, virtual markers were placed on the animated bone models at the attachment points of representative fibers and the whole muscle length measured as the change in distance between these markers (Fig. 2B). Muscle length was normalized to its mean initial length prior to the onset of the strike (L_i). For each muscle, whole-muscle velocity was calculated at each time step as the change in muscle length divided by the change in time, and expressed in L_i s^{-1}, with shortening indicated by positive velocities.

Power and work calculations

Following the methods of Camp et al. (2015), instantaneous suction expansion power was estimated in MATLAB as the product of the rate of volume change (m^3 s^{-1}) and buccal cavity pressure (Pa). Buccal pressure was filtered (low-pass Butterworth, 60 Hz cutoff), resampled from 1000 Hz to 500 Hz to match the frequency of the volume data, and expressed relative to the initial, ambient pressure prior to the strike. At each time step the current and subsequent pressure values were averaged and multiplied by −1, so that the product of subambient pressures and increasing volume rates resulted in positive power. The work of suction expansion was calculated as the integral (via the trapezoidal method) of the power–time curve for each strike.

These work and power estimates have two main sources of error. First, they neglect the additional power and work required to overcome the drag and inertia of accelerating the feeding apparatus

Journal of Experimental Biology (2018) 221, jeb178160. doi:10.1242/jeb.178160

Table 1. Mean timing and magnitude of peak muscle strain, velocity during the period of peak power, and bilateral muscle mass for each individual

Muscle	Variable	Bluegill 1 (*N*=6)	Bluegill 3 (*N*=5)
Epaxials	Strain[a] (%)	3.9 (0.5)	4.4 (0.9)
	Time[b] of peak strain (ms)	4.3 (1.5)	10.8 (2.2)
	Velocity[c] (L_i s^{-1})	2.2 (0.3)	1.9 (0.5)
	Mass (g)	26.4	26.2
Hypaxials	Strain[a] (%)	6.8 (0.6)	5.5 (0.9)
	Time[b] of peak strain (ms)	8.7 (2.0)	12.0 (6.1)
	Velocity[c] (L_i s^{-1})	3.4 (0.2)	2.1 (0.6)
	Mass (g)	14.8	13.1
Levator arcus palatini	Strain[a] (%)	10.1 (0.9)	5.7 (1.2)
	Time[b] of peak strain (ms)	39.7 (7.1)	39.6 (5.0)
	Velocity[c] (L_i s^{-1})	1.4 (0.7)	−0.45 (0.5)
	Mass (g)	0.20	0.22
Dilator operculi	Strain[a] (%)	8.5 (1.1)	10.6 (2.2)
	Time[b] of peak strain (ms)	41.3 (6.5)	44.0 (4.3)
	Velocity[c] (L_i s^{-1})	2.1 (0.8)	−1.9 (1.1)
	Mass (g)	0.10	0.10
Levator operculi	Strain[a] (%)	6.9 (1.1)	7.3 (0.9)
	Time[b] of peak strain (ms)	10.3 (1.8)	7.6 (2.3)
	Velocity[c] (L_i s^{-1})	3.2 (1.0)	3.3 (0.6)
	Mass (g)	0.06	0.10
Sternohyoideus	Strain[a] (%)	12.0 (1.0)	4.4 (1.2)
	Time[b] of peak strain (ms)	11.3 (1.3)	−3.6 (12.7)
	Velocity[c] (L_i s^{-1})	4.4 (0.5)	1.4 (0.7)
	Mass (g)	1.5	2.4

[a]Magnitude of peak muscle strain [% initial length (L_i); positive values indicate shortening].
[b]Time relative to the time of peak gape.
[c]Velocity during the period of peak power (positive values indicate shortening).
For each individual, mean values are shown, with s.e.m. shown in parentheses.

(Van Wassenbergh et al., 2015), and the inertia of shortening muscle masses. This omission is most likely to result in our values underestimating the actual work and power required to expand the mouth. Based on inverse dynamic models of suction feeding, which calculated the pressure–volume power as well as the power required to overcome drag and inertia, we expect this underestimate to be less than 5–10% (Aerts et al., 1987; Muller et al., 1982; Van Wassenbergh et al., 2015). Second, our power estimates are based on a single measurement of pressure, which does not capture the spatial variation of intraoral pressure (Muller et al., 1982). A computational fluid dynamics (CFD) model of a bluegill sunfish performing a single, low-power suction strike found that using a single pressure value (the mean pressure in the buccal cavity) resulted in an overestimate of peak instantaneous suction power (4.5 instead of 3 mW) (Van Wassenbergh, 2015). However, it is unclear whether this can be extrapolated to the higher-power strikes used in this study, or how the assumptions of this CFD model – for example, modeling the buccal cavity as a radially symmetric, expanding cone – may also influence peak power calculations. Therefore, it is difficult to determine the likely magnitude or direction of error resulting from the use of a single pressure measurement to estimate power in this study.

For each fish, the four cranial muscles (including the sternohyoideus) and two axial muscles were dissected out post-mortem, unilaterally, and weighed on a digital scale. Only the regions of the epaxials and hypaxials that consistently shortened during suction feeding (Fig. 1A, and see 'Muscle length changes' section for detailed description) were included in the mass measurements. Unilateral masses were doubled to calculate the bilateral mass of each muscle (Table 1). Suction expansion power and work were divided by the total axial muscle mass involved in shortening to estimate the axial mass-specific power and work output of each strike. Similarly, the cranial mass-specific power and work outputs were estimated by dividing the power and work of suction expansion by the total cranial muscle mass (the summed bilateral mass of all four muscles).

RESULTS

Measurements of buccal cavity volume change and pressure were used to estimate the power and work required for suction-feeding strikes. To determine the role of each cranial (including the sternohyoideus) and axial muscle in generating that power and work, we measured muscle mass, length and instantaneous velocity. Muscles can only generate power by actively shortening. As all cranial and axial muscles studied here are known to be active during suction feeding in sunfish (Lauder and Lanyon, 1980), we used measurements of muscle shortening to infer which cranial muscles and regions of axial muscles generated power during suction expansion. Both individuals studied showed broadly similar patterns but variable magnitudes in their kinematics, muscle shortening and buccal cavity expansion, so we report individual means and standard errors (*N*=6 strikes for bluegill 1; *N*=5 for bluegill 3) below and in Tables 1, 2, and Table S1.

Axial muscle function

Large regions of the epaxial and hypaxial muscles shortened during suction feeding to elevate the neurocranium and retract the pectoral girdle, respectively. Relative to the body plane, the neurocranium elevated (positive *z*-axis rotation) by a mean peak of 11.9±1.6 deg in bluegill 1 and 13.7±2.1 deg in bluegill 3, whereas rotations about the other axes were generally smaller and highly variable (Fig. 3B; Table S1). The cleithrum retracted (negative *z*-axis rotation) relative to the body plane by a mean peak of −7.1±0.7 deg in bluegill 1 and −4.6±1.0 deg in bluegill 3, and showed a tendency for small rotations about the other two axes (Fig. 3B). Neither bone had substantial translations (Table S1). Neurocranium elevation and

Journal of Experimental Biology (2018) 221, jeb178160. doi:10.1242/jeb.178160

Table 2. Mean timing and magnitude of peak pressure, volume, power and work of suction-feeding strikes, along with body and summed, bilateral muscle masses

Parameter	Variable	Bluegill 1 (*N*=6)	Bluegill 3 (*N*=5)
Pressure	Minimum pressure (kPa)	−32.2 (2.2)	−17.2 (4.6)
	Time[a] of minimum pressure (ms)	−1.7 (2.3)	−10.8 (1.9)
Volume	Volume (cm^3)	18.3 (1.0)	18.4 (1.0)
	Time[a] of peak volume (ms)	12.7 (1.6)	14.4 (2.7)
	Volume rate ($cm^3\ s^{-1}$)	386.5 (58.2)	351.2 (74.9)
	Time[a] of peak volume rate (ms)	−5.3 (2.6)	−5.2 (2.2)
Power	Power (W)	11.4 (2.1)	5.2 (2.1)
	Time[a] of peak power (ms)	−4.3 (2.6)	−9.2 (1.4)
Work	Work (J)	0.14 (0.03)	0.07 (0.02)
Mass	Total body (g)	164	162
	All cranial muscles (g)	1.86	2.84
	All axial muscles (g)	41.1	39.12

[a]Time relative to time of peak gape.
For each individual, mean values are shown, with s.e.m. shown in parentheses.

pectoral girdle retraction were the result of epaxial and hypaxial (respectively) muscle shortening. In both muscles, shortening extended over halfway down the body (shaded region in Fig. 1A; see also Fig. S1). Across this entire superficial muscle region where shortening was measured (defined as the whole-muscle length), maximum longitudinal shortening of the epaxial muscle mass reached a mean of 3.9±0.5% (bluegill 1) and 4.4±0.5% (bluegill 3) of initial length, and maximum hypaxial shortening reached a mean of 6.8±0.6% (bluegill 1) and 5.5±0.9% (bluegill 3) of initial length (Fig. 4, Table 1). Mean epaxial muscle shortening velocity during the period of peak power output (i.e. when expansion power was within 25% of its maximum) was 2.2±0.3 $L_i\ s^{-1}$ (bluegill 1) and 1.9±0.5 $L_i\ s^{-1}$ (bluegill 3). For the hypaxials, mean shortening velocity during peak power was 3.4±0.2 $L_i\ s^{-1}$ (bluegill 1) and 2.1±0.6 $L_i\ s^{-1}$ (bluegill 3).

Cranial muscle function

The largest of the head muscles examined in this study, the sternohyoideus, consistently shortened and contributed to retraction and depression of the urohyal. Relative to the body plane, the urohyal translated caudally (negative *x*-axis) and ventrally (negative *y*-axis), with little mediolateral translation or rotation (*z*-axis) of this mid-sagittal bone (Fig. 3C; Table S1). Although the sternohyoid is not the only muscle that can contribute to urohyal translation, sternohyoid muscle shortening usually coincided with urohyal retraction (Fig. 5). Over its whole length, the sternohyoideus shortened by a mean of 12±1% in bluegill 1 and 4.3±1.2% in bluegill 3 (Fig. 4, Table 1), and had a mean shortening velocity of 4.4±0.5 $L_i\ s^{-1}$ (bluegill 1) and 1.4±0.7 $L_i\ s^{-1}$ (bluegill 3) during peak power. Of the remaining cranial muscles, only the levator operculi consistently shortened during peak expansion power, with a mean maximum strain of 6.9±1.1% (bluegill 1) and 7.3±0.9% (bluegill 3), and mean shortening velocity of 3.2±1.0 $L_i\ s^{-1}$ (bluegill 1) and 3.3±0.6 $L_i\ s^{-1}$ (bluegill 3) during peak power. The dilator operculi and the levator arcus palatini muscles maintained a fairly constant length – or even lengthened – during peak expansion power, and only started to shorten after peak expansion power occurred (Fig. 4).

Suction expansion power and work

The mouth expansion generated by these muscle strains and skeletal kinematics resulted in subambient pressures and rapid volume changes in the buccal cavity, and generally required substantial power. Subambient pressures varied across strikes, with peak values from −12 to −38 kPa, and the rate of mouth volume change reached a mean maximum of 387±58 $cm^3\ s^{-1}$ in bluegill 1 and 351±75 $cm^3\ s^{-1}$ in bluegill 3 (Table 2). Peak expansion power occurred about 5–10 ms before peak gape (Fig. 5, Table 2). The magnitude of peak power ranged from 0.55 to 18 W across all measured strikes (Fig. 6). When expressed as power per unit axial (i.e. summed hypaxial and epaxial) muscle mass, the resulting mass-specific peak powers ranged from 14 to 438 W kg^{-1} (mean 277±51 W kg^{-1} for bluegill 1 and 133±54 W kg^{-1} for bluegill 3) (Fig. 6). When the peak expansion powers were expressed as power per unit cranial (including the sternohyoideus) muscle mass, mass-specific powers ranged from 192 to 9691 W kg^{-1} (mean 6126±1127 W kg^{-1} for bluegill 1 and 1832±740 W kg^{-1} for bluegill 3) (Fig. 6).

The work required for each mouth expansion event was estimated as the area under the power–time curve, and expressed per unit axial muscle mass and per unit cranial muscle mass (Figs 7, 8). The axial mass-specific expansion work had a range of 0.24–5.6 J kg^{-1} (Fig. 8B), and a mean of 3.3±0.7 J kg^{-1} for bluegill 1 and 1.9±0.6 J kg^{-1} for bluegill 3 (Table 2). Cranial mass-specific expansion work ranged from 3.4 to 124 J kg^{-1}, with a mean of 73±14.6 J kg^{-1} for bluegill 1 and 26.1±8.5 J kg^{-1} for bluegill 3 (Table 2). For comparison, we also calculated the absolute and axial mass-specific expansion work of largemouth bass using previously collected data (Camp et al., 2015). The absolute expansion work ranged from 0.015 to 0.48 J across all recorded strikes from the three bass (Fig. 8A). Mean axial mass-specific work was 0.36±0.08, 2.5±0.4 and 0.85±0.01 for bass 1 (*n*=10 strikes), bass 2 (*n*=9 strikes) and bass 3 (*n*=10 strikes), respectively (Fig. 8B).

DISCUSSION

Bluegill sunfish generated large subambient pressures and rapid volume changes in the buccal cavity to produce powerful strikes. Buccal pressures were similar to those reported previously (Carroll and Wainwright, 2009; Higham et al., 2006a) and the mean peak rate of volume change was about 1.5 times more than previously reported for similarly sized sunfish (Higham et al., 2006b). Of the four head muscles examined, the sternohyoideus and levator operculi muscles consistently shortened during peak expansion power. However, these muscles were too small to directly generate meaningful amounts of power, and we found no evidence of power amplification through elastic energy storage in these or any other muscles. Instead, sunfish relied on high power outputs from their axial muscles. These muscles shortened across the same region as largemouth bass – from the head to over halfway down the body (Camp and Brainerd, 2014) – but with substantially higher estimated muscle mass-specific power outputs of up to

Journal of Experimental Biology (2018) 221, jeb178160. doi:10.1242/jeb.178160

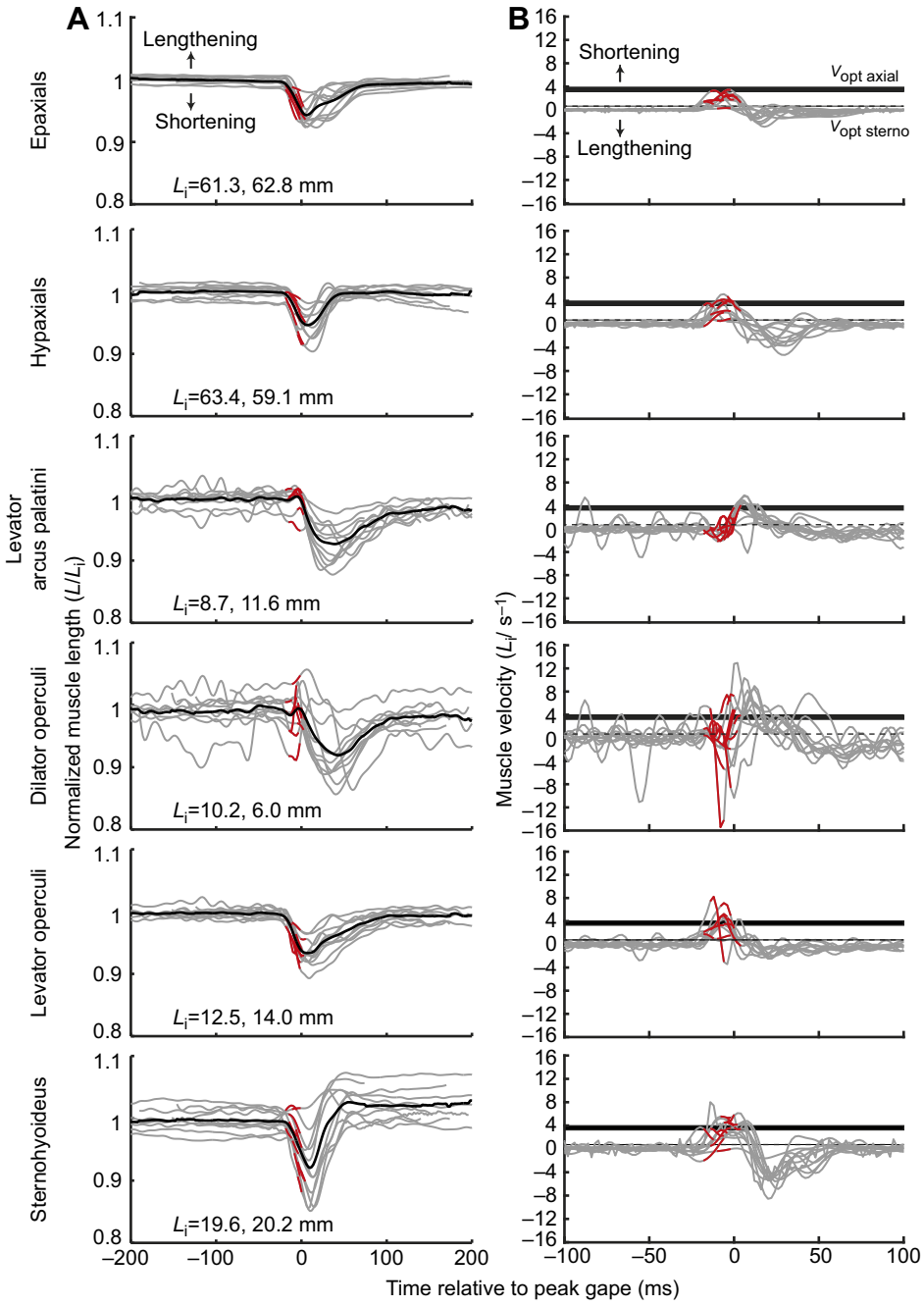

Fig. 4. Normalized muscle length and velocity during suction feeding. (A,B) Traces from individual strikes (gray lines) are shown, with the values during peak (within 25% of maximum) expansion power highlighted (red lines). (A) Length of each muscle normalized to its mean initial muscle length (L_i), with L_i values listed for bluegill 1 and bluegill 3, respectively. Decreasing values indicate shortening. The mean length at each time point (across all strikes and both individuals; N=11 strikes) is also shown for each muscle (black lines). (B) Instantaneous velocity of each muscle, with the optimum velocity for power production of the sternohyoideus ($V_{opt\ sterno}$; dashed line) and the axial muscles ($V_{opt\ axial}$; solid bar), which spans the V_{opt} measured for epaxial and 'myotomal' muscles (Carroll et al., 2009). Note that, for velocity, positive values indicate shortening.

300–438 W kg^{-1} (Fig. 6). Both species generated absolute peak expansion powers of 10–15 W during suction feeding (Fig. 6; Camp et al., 2015), but the sunfish in this study produced these strikes with less than half the axial muscle mass of the larger bass individuals from our prior study (Camp et al., 2015). Sunfish axial muscles also shortened at faster velocities than those of bass and may have been nearer the optimum for power production (Carroll et al., 2009), which likely contributed to the higher power output of these muscles. We conclude that bluegill sunfish rely on high power outputs from the axial muscles to generate fast and forceful suction-feeding strikes.

Cranial muscle function

In bluegill sunfish, two cranial muscles – the sternohyoideus and levator operculi – consistently shortened during peak expansion power (Fig. 4). Although muscle power was not measured directly, we infer that muscle shortening indicates power production because these muscles are known to be active during suction expansion (Lauder and Lanyon, 1980; Lauder et al., 1986). Additionally, the skeletal motions produced by these shortening muscles occur against inertial and hydrodynamic resistance, and therefore require power. The levator operculi shortened by about 7% in both individuals, presumably elevating (i.e. dorsally rotating in a parasagittal plane) the operculum. This motion may not directly expand the mouth, but can be transmitted through the opercular linkage, a set of bones and ligaments, to contribute to lower-jaw depression (Ballintijn, 1969; Liem, 1980). In largemouth bass, the levator operculi's shortening holds the operculum in place relative to the body – against resistance from the suspensorium – and allows epaxial-powered neurocranium elevation to be transmitted through

Journal of Experimental Biology (2018) 221, jeb178160. doi:10.1242/jeb.178160

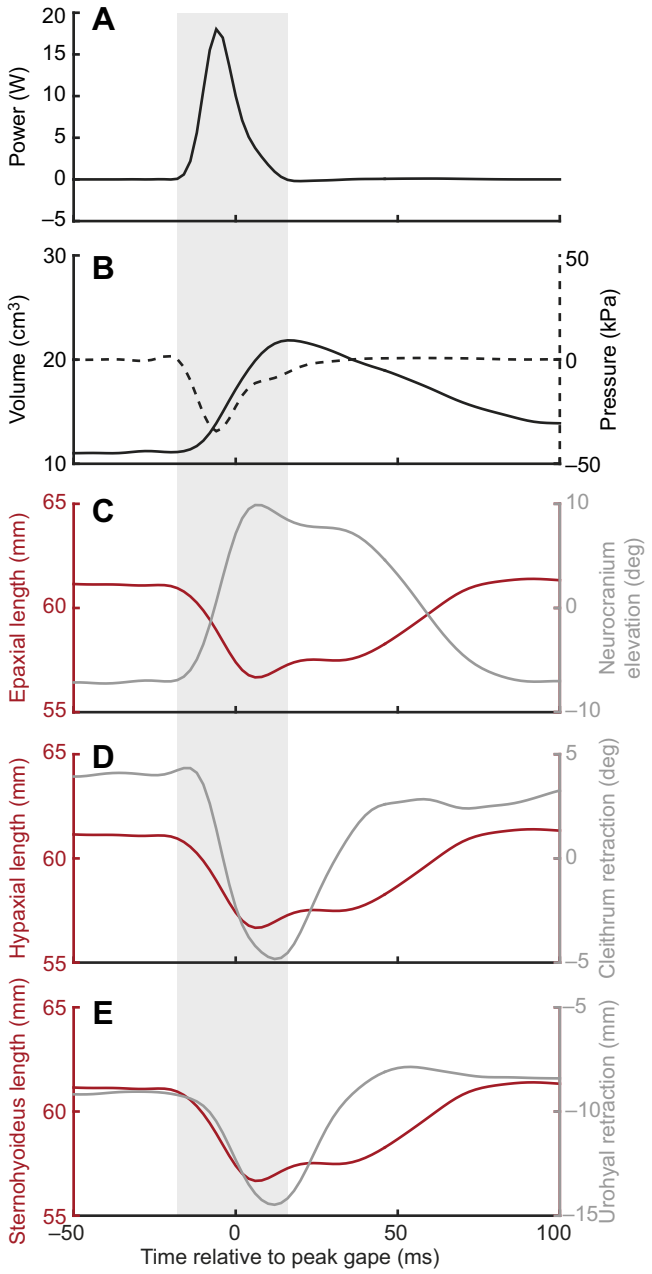

Fig. 5. Expansion power, muscle length and skeletal kinematics from the most powerful sunfish strike recorded (bluegill 1). Power (A) is estimated from the product of buccal pressure (B) and rate of bilateral mouth volume change (note that absolute volume is shown in B). Whole-muscle lengths of the epaxial (C), hypaxial (D) and sternohyoideus (E) are shown in mm, and not relative to initial lengths. Neurocranium elevation (C), cleithrum retraction (D) and urohyal retraction (E) are measured relative to the body plane, and again magnitudes are not relative to initial values. The gray bar indicates the period of power production. Note that the onset of muscle shortening and corresponding skeletal motion are generally coincident, indicating an absence of muscle shortening prior to power production.

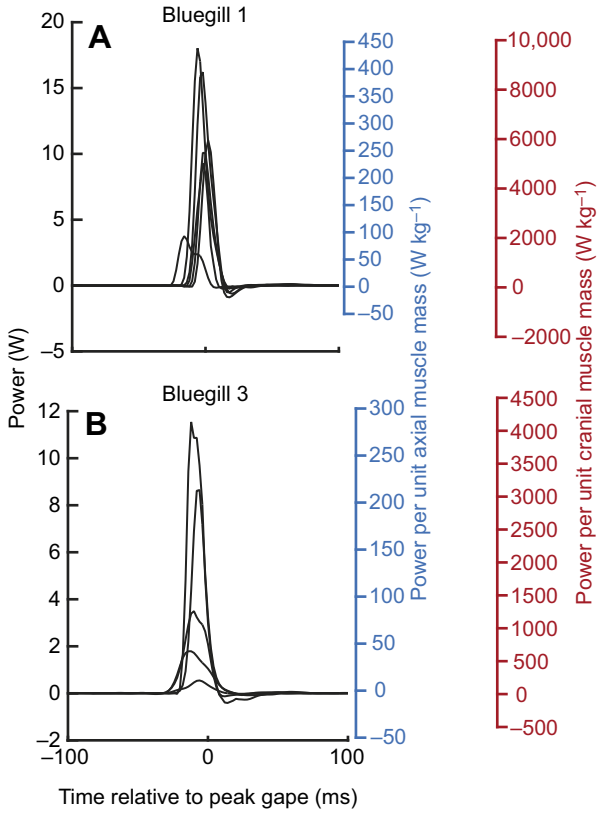

Fig. 6. Suction expansion power for each strike. (A) Bluegill 1. (B) Bluegill 3. The absolute magnitude of power (W) estimated for expansion is shown in black on the left *y*-axis, graphed as a function of time. The two right *y*-axes express these same power magnitudes as mass-specific power (W kg^{-1}) by dividing the estimated expansion power by the total mass of the axial muscles (blue axis) or by the total mass of the four cranial muscles (red axis) of each individual. These mass-specific powers represent the estimated power outputs the axial or cranial muscles would have to generate, assuming they were the sole source of power for suction expansion.

this linkage to the lower jaw (Camp and Brainerd, 2015). Thus, even when cranial muscles are generating power, they can still function to transmit axial muscle power. As in largemouth bass, the levator operculi shortened relatively quickly and reached a mean peak velocity of about 3 lengths (L_i) s^{-1}, which actually exceeds the optimum velocities for power production (~1.6 L_i s^{-1}) calculated for the sternohyoideus muscle of sunfish (Carroll et al., 2009). The levator operculi of bluegill sunfish may have a similar role to that of bass during suction feeding (Camp and Brainerd, 2015), but further study of the opercular kinematics is needed to confirm this.

The sternohyoideus muscle shortened to retract the urohyal and hyoid apparatus (Fig. 5E), as predicted by Lauder and Lanyon (1980). However, in contrast to the hypothesized function proposed by these authors, the hypaxial muscles also shortened at the same time to retract the cleithrum (Fig. 5D). As these muscles are in series (Fig. 1A) and both active during suction feeding, it was proposed that the hypaxials produce only force to hold the pectoral girdle immobile and provide a stable attachment site for the sternohyoideus to shorten against (Lauder and Lanyon, 1980). In largemouth bass and clariid catfishes, the only other species where both muscle lengths have been measured, the opposite occurred: the hypaxials shortened while the sternohyoideus maintained a relatively constant length or was stretched as it transmitted hypaxial power to the hyoid (Camp and Brainerd, 2014; Van Wassenbergh et al., 2005, 2007). Our data from bluegill sunfish are the first empirical evidence of both muscles shortening during peak expansion power to generate positive power for hyoid retraction and depression. The sternohyoideus muscle in bluegill 1 shortened relatively quickly, with mean peak velocities of about 4 L_i s^{-1}, exceeding the optimum velocity for power production (~1.6 L_i s^{-1})

Journal of Experimental Biology (2018) 221, jeb178160. doi:10.1242/jeb.178160

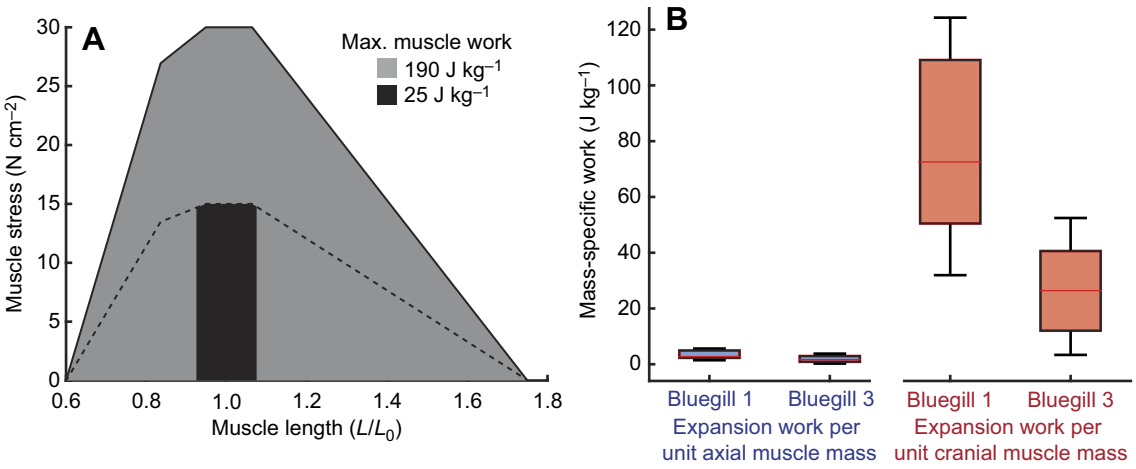

Fig. 7. Estimated muscle work capacity and mass-specific work of expansion during sunfish suction feeding. (A) Vertebrate muscle length tension curve (redrawn from Peplowski and Marsh, 1997 and assuming a maximum isometric force of 30 N cm^{-2}). Theoretical work capacity (J kg^{-1}) of the muscle was calculated as the area under the curve, divided by the density of vertebrate muscle [1.06×10^{9} kg cm^{-3} (Mendez and Keys, 1960)], and finally divided by 100 to convert from N cm kg^{-1} to N m kg^{-1} so that the final value is in J kg^{-1}. Assuming that the muscle shortens infinitely slowly and with 115% strain, i.e. from 175% of its optimal length (L_0) to 60% of its optimal length, it could produce 190 J kg^{-1} of work (gray shaded area and solid line). A more realistic estimate of maximum work capacity is shown by the black shaded region (25 J kg^{-1}), which assumes only a 15% strain (based on *in vivo* shortening measured in this study) and that the rapid muscle shortening required for powerful feeding will result in a 50% reduction in force (dashed line) due to force–velocity effects (Peplowski and Marsh, 1997). (B) The estimated mass-specific work of suction expansion, calculated as the area under the power–time curve for each strike, divided by the mass of the axial muscles (blue; left-side boxplots) or by the mass of the cranial muscles (red; right-side boxplots). Each boxplot shows the mean (red line), the 25–75% percentile (box edges) and extreme values (whiskers) of mass-specific work required for each individual (*N*=6 strikes for bluegill 1; *N*=5 strikes for bluegill 3), assuming only the axial (left-hand bars) or cranial (right-hand bars) muscles produce the work of suction.

calculated for this muscle in similarly sized sunfish (Carroll et al., 2009), although, in bluegill 3, it shortened more slowly (1.4 L_i s^{-1}).

Cranial muscle power and work

Although the sternohyoideus and levator operculi did shorten during peak expansion power, the power output from these small muscles would have been negligible compared to that required for most suction strikes. These and the other cranial muscles together would have needed power outputs of up to 9691 W kg^{-1} to directly power suction expansion by themselves (Fig. 6), which far exceeds the maximum recorded from or any vertebrate muscle [1121 W kg^{-1} (Askew and Marsh, 2001)]. Even assuming the relatively high muscle mass-specific power output of 438 W kg^{-1} inferred for the axial muscles, the sternohyoideus muscle could not have generated more than 1 W of power or 5–10% of the peak power required for the most powerful strikes. Put another way, including the sternohyoideus muscle mass – by far the largest of the four cranial muscles examined – with the axial muscles would only lower the maximum power output estimated for the axial muscles from 438 to 422 W kg^{-1}. The muscles of the head likely make important contributions to suction-feeding kinematics (see above), but are not a major source of direct muscle power for bluegill sunfish.

Additionally, we found no evidence that the bluegill sunfish's cranial muscle power was amplified by elastic energy storage prior to suction expansion. Such power amplification mechanisms are usually associated with muscle shortening and activation prior to skeletal motion (Astley and Roberts, 2012; Van Wassenbergh et al., 2008), but we did not observe any muscle shortening prior to suction expansion in sunfish (Fig. 4, Table 1), even during the most powerful strike (Fig. 5), nor have the cranial muscles been reported to activate prior to suction expansion in bluegill sunfish (Lauder and Lanyon, 1980; Lauder et al., 1986). Moreover, such elastic energy storage would still require the cranial muscles to generate the work for suction expansion. We estimated that the cranial muscles have the potential to generate about 25 J kg^{-1} of work under the conditions observed in suction feeding (Fig. 7A), but most suction strikes would have required at least 40–60 J kg^{-1} of work from these muscles (Fig. 7B). These work estimates follow the work capacity calculations of Peplowski and Marsh (1997), and assume a maximum isometric muscle stress of 30 N cm^{-2}, a 50% decrease in force due to force–velocity effects during rapid shortening, and that the muscles shorten by 15% of their initial length [the maximum shortening measured in this study (Fig. 4)]. The small mass of the cranial muscles in bluegill sunfish limits the work and power they can contribute to suction-feeding strikes.

Axial muscle power and work

As the cranial muscles could generate relatively little power or work, we conclude that bluegill sunfish relied almost exclusively on the large axial muscles to generate powerful suction-feeding strikes. Despite their different (i.e. shorter and deeper) body shape, sunfish shortened epaxial and hypaxial muscles over the same region as bass: from the muscles' cranial attachment sites on the neurocranium and pectoral girdle to the caudal edge of the first dorsal fin and the rostral edge of the anal fin, respectively (Fig. 1A). It is interesting that the magnitude of shortening was not distributed evenly across the axial muscle of sunfish (Fig. S1), as in bass (Camp and Brainerd, 2014), but the functional implications of this remain unclear. Muscle activity has only been measured and confirmed via electromyography in the most rostral portion of these muscles during suction feeding in sunfish (Lauder and Lanyon, 1980), but we presume these regions actively shortened. Axial muscle shortening contributes directly to dorsoventral expansion of the buccal cavity by elevating the neurocranium and retracting the pectoral girdle (Fig. 3) against suction pressure and inertial forces (Van Wassenbergh et al., 2015). These skeletal motions also allow axial muscle power to be transmitted to the rest of the skull, via

Journal of Experimental Biology (2018) 221, jeb178160. doi:10.1242/jeb.178160

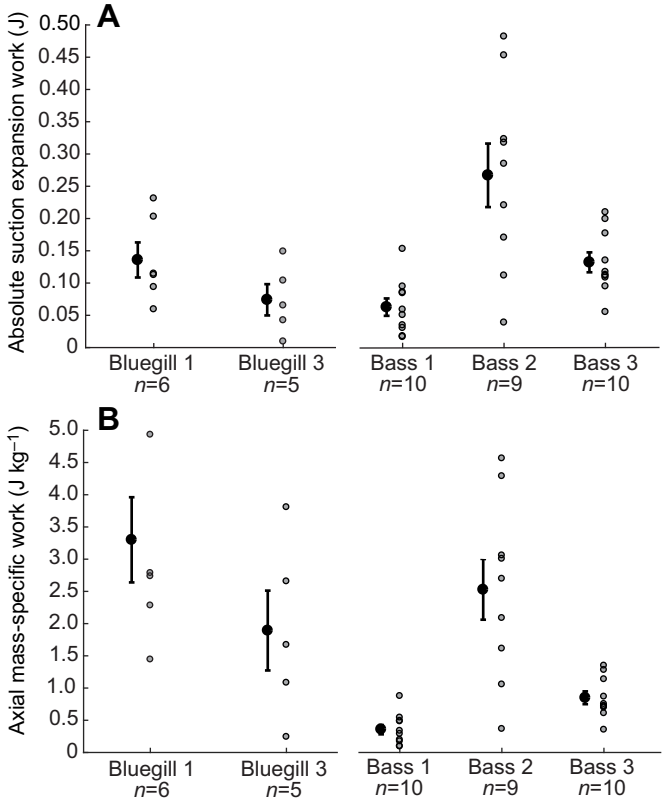

Fig. 8. Estimated expansion work in bluegill sunfish (from this study) and largemouth bass (data from Camp et al., 2015). (A) Absolute magnitude of suction expansion work during feeding strikes. (B) The same suction expansion work, expressed per unit axial muscle mass, i.e. the summed mass of the hypaxial and epaxial muscles. In both panels, for each individual, the expansion work is shown for each strike (gray filled circles) along with the mean expansion work (filled black circle) and s.e.m. (black lines) for that individual. The number of strikes, from which means and standard errors were calculated, are listed beneath each individual. Bluegill mean axial mass-specific work is the same as that shown in Fig. 7, but included here for comparison with largemouth bass.

musculoskeletal linkages, to generate the full, 3D expansion of the buccal cavity. These results further emphasize the role that hypaxial muscles and pectoral girdle retraction can play in powering suction feeding and expanding the mouth cavity. Although the potential for contribution of epaxial muscles to suction feeding has been recognized (e.g. Carroll and Wainwright, 2009; Lauder and Lanyon, 1980), the role of hypaxial muscles has received less attention (e.g. Carroll and Wainwright, 2009).

Bluegill sunfish relied on high power-outputs from their axial muscles – rather than recruiting a larger region of axial muscles or generating power from more cranial muscles – to meet the mechanical demands of suction feeding. The sunfish in this study generated similar absolute peak expansion powers (up to 18 W) as the largemouth bass (up to 15 W) from our previous study, even though the sunfish were shorter (standard length of ∼170 mm compared with ∼300 mm for bass) and had a total mass of shortening axial muscle only 30–40% of the axial muscle mass of bass (Table 2; Camp et al., 2015). Therefore, the most powerful bass strike needed only 141 W kg^{-1} of axial muscle power output (Camp et al., 2015), whereas the axial muscle of sunfish was estimated to generate 438 W kg^{-1} for the most powerful strike (Fig. 6). High instantaneous power outputs are not unexpected for these white-, fast-fibered muscles, which fish also use for powerful escape behaviors, i.e. C-starts (Frith and Blake, 1995; Rome et al., 1988). Even the highest muscle power output estimated here (438 W kg^{-1}) is within the maximum measured from fish axial muscle with *in vitro* work loops (Altringham et al., 1993) and other vertebrate muscles (Askew and Marsh, 2001; Curtin et al., 2005). As it is unlikely that we captured the maximum suction-feeding performance of bluegill sunfish, especially given our relatively small sample size (e.g. Astley et al., 2013), the maximum power outputs of these muscles could be even higher. However, our axial mass-specific power outputs should be interpreted with some caution as they are based on expansion power estimates with their own sources of error (see Materials and Methods), and not direct measurements of muscle power production. For most strikes, our estimated axial muscle mass-specific power outputs are at or below the maximum power output of 300 W kg^{-1} (Fig. 6) previously estimated for bluegill sunfish (Carroll and Wainwright, 2009).

The shortening velocities measured from the axial muscles are consistent with these muscles operating at or near their maximum power production. The epaxials and hypaxials shortened at 2–3 initial lengths (L_i) s^{-1} during peak expansion power (Table 1), approaching the optimum velocity (V_{opt}) of power production of 3.3 or 4 L_i s^{-1} for 'myotomal' and epaxial muscle (Fig. 4B), respectively, of similarly sized bluegill sunfish (Carroll et al., 2009). The axial muscles of largemouth bass shortened much more slowly (0.5–1.6 L_i s^{-1}), both compared with sunfish and to the V_{opt} of 4 L_i s^{-1} measured for this species (Carroll et al., 2009; Coughlin and Carroll, 2006). We hypothesize that sunfish may achieve higher mass-specific power outputs from their axial muscles, compared to bass, by shortening these muscles at speeds near the optimum for power production. However, shortening velocity is just one component of muscle power, and measurements of muscle activation, force production and fiber length dynamics are needed to better understand power production in these muscles.

Additionally, our measurements of longitudinal axial muscle shortening velocity may not be representative of fiber-level strains across the entire volume of the hypaxials and epaxials. Whole-muscle velocity was measured across superficial regions near the midsagittal plane. In reality, the magnitude and velocity of shortening may vary throughout these muscles as a result of the complex fiber orientation of the axial muscles (Alexander, 1969; Gemballa and Vogel, 2002) and/or the distance from the neutral axis of cranial/pectoral rotation. For example, during swimming the muscle fibers furthest from the neutral axis of bending (i.e. the vertebral column) would be expected to shorten more quickly than those closest to the neutral axis, if the body bends like a simple homogenous beam (Shadwick et al., 1998), and yet muscle fiber orientations act to homogenize fiber-level strain during swimming (Azizi and Brainerd, 2007; Rome and Sosnicki, 1991). Although our velocity measurements may therefore not be representative of the entire muscle, the high powers measured for the entire musculature [near or even above their measured maximum of 300 W kg^{-1} (Carroll et al., 2009)] would seem to support the idea that fibers throughout the axial muscles are shortening at near optimal velocities for power production.

It is also possible that some kind of elastic energy storage mechanism is used to amplify axial muscle power, particularly during the most powerful strikes. The estimated work of suction expansion was well within the expected work capacity of the axial muscles, requiring outputs of no more than 6 J kg^{-1} (Figs 7, 8), so these muscles could be using mechanisms to amplify the rate of energy production, i.e. power. While we found no evidence of catapult-style power amplification [such as active muscle shortening

prior to suction expansion and axial muscles with long tendons, as in pipefishes (Van Wassenbergh et al., 2014, 2008)], these muscles may be using a subtler mechanism. For example, energy generated at the beginning of shortening could be stored in connective tissues or myoseptal tendons and then released later in the contraction to amplify peak power. However, further measurements of axial fiber activation and lengths – rather than the whole-muscle lengths recorded here – and force outputs are needed to test this.

In contrast to the high mass-specific muscle power output (Fig. 6), the mechanical work required for these bluegill sunfish strikes was more similar to that of the largemouth bass from our previous study (Fig. 8). The absolute work of suction expansion – the product of pressure and volume or the integral of the power–time curve – in sunfish strikes was similar or less than that of bass (Fig. 8A). The maximum work recorded from a sunfish strike (0.25 J) was about half the maximum observed in the bass (0.50 J), although there was considerable overlap in the range of expansion work for both species (Fig. 8A). As the absolute peak expansion power was similar between sunfish and bass, this difference in expansion work may reflect a greater duration of suction expansion in bass. For example, in the sunfish strike shown in Fig. 5, positive power is generated over about 30 ms, whereas, in the bass strike shown in figure 3 of Camp et al. (2015), positive power occurs over about 60 ms. The bluegill sunfish strikes measured in this study had similar or slightly higher mass-specific work outputs for the axial muscles than those of the largemouth bass measured previously (Fig. 8B): average axial mass-specific work was 0.36–2.5 J kg^{-1} (depending on the individual) in largemouth bass compared with 1.8 and 3.4 J kg^{-1} in bluegill 1 and 3, respectively (Fig. 7, Table 2). Thus, the axial muscles of sunfish had to generate only somewhat higher work outputs but much higher power outputs than bass to generate suction expansion. Conversely, the slower axial muscle shortening velocities measured in bass may be related to slower mouth expansion, and the need for these muscles to generate work but not particularly high power outputs.

Concluding remarks

Our results show that bluegill sunfish rely on high power outputs from their axial muscles to meet the challenge of powerful feeding as a small-mouthed, deep-bodied, suction-reliant species. Largemouth bass strikes also required power from the axial muscles but, in sunfish, large regions of axial musculature had to operate at or near maximum power output to produce the most powerful suction strikes observed. Although this supports the presence of axial-powered feeding in a broader range of fishes beyond those with bass-like body shapes, it also highlights how the use of axial power may vary with body shape as well as feeding behavior. Together with previous studies, these results demonstrate that we must take feeding functions into account in order to understand the morphology, physiology and evolution of these body muscles in fishes. While the axial muscles can generate the power for suction expansion, it is the cranial muscles and skeleton that generate the 3D motion and anterior-to-posterior progression of suction expansion. These functions are no less important than power generation, and may be achieved with or without muscle shortening during peak expansion power. For example, the sternohyoideus muscle shortens to generate power in bluegill sunfish, but maintains a constant length in bass to transmit hypaxial muscle power. A major challenge remains to understand how the muscles of the head, together with the complex cranial skeleton, transmit axial muscle power and control suction-feeding kinematics.

Acknowledgements

We are grateful to the many members of the Brown EEB Morphology Group whose assistance made this work possible, including E. Giblin, J. Lomax, J. Laurence-Chasen and N. Chen (fish surgery and X-ray filming); D. Sleboda, P. Feltman and K. Rivard (specimen collection); S. Gatesy (dynamic digital endocast method); and R. Kambic (skeletal animation techniques). We also appreciate the CT scanning facilities provided by the Karl F. Liem Bioimaging Center at Friday Harbor Laboratories, University of Washington.

Competing interests

The authors declare no competing or financial interests.

Author contributions

Conceptualization: A.L.C., T.J.R., E.L.B.; Formal analysis: A.L.C., T.J.R., E.L.B.; Investigation: A.L.C.; Writing - original draft: A.L.C.; Writing - review & editing: A.L.C., T.J.R., E.L.B.; Visualization: A.L.C.; Supervision: T.J.R., E.L.B.

Funding

This work was supported by the National Science Foundation [IOS-1655756 to E.L.B. and A.L.C., DBI-1661129 to E.L.B., and IOS-1354289 to T.J.R.], a Brown University EEB Doctoral Dissertation Development Grant [A.L.C.], and the Bushnell Graduate Research and Education Fund [A.L.C.].

Data availability

Data are available on the XMA Portal (xmaportal.org) in the study 'Sunfish suction feeding', with the identifier BROWN48.

Supplementary information

Supplementary information available online at
http://jeb.biologists.org/lookup/doi/10.1242/jeb.178160.supplemental

References

Aerts, P., Osse, J. W. M. and Verraes, W. (1987). Model of jaw depression during feeding in *Astatotilapia elegans* (Teleostei: Cichlidae): mechanisms for energy storage and triggering. *J. Morphol.* **194**, 85-109.

Alexander, R. (1967). Feeding. In *Functional Design in Fishes* (ed. A. J. Cain), pp. 89-114. London: Hutchinson and Co.

Alexander, R. M. N. (1969). The orientation of muscle fibres in the myomeres of fishes. *J. Mar. Biol. Assoc. UK* **49**, 263-290.

Alexander, R. (1970). Mechanics of the feeding action of various teleost fishes. *J. Zool.* **162**, 142-156.

Altringham, J. D., Wardle, C. S. and Smith, C. I. (1993). Myotomal muscle function at different locations in the body of a swimming fish. *J. Exp. Biol.* **182**, 191-206.

Askew, G. N. and Marsh, R. L. (2001). The mechanical power output of the pectoralis muscle of blue-breasted quail (*Coturnix chinensis*): the in vivo length cycle and its implications for muscle performance. *J. Exp. Biol.* **204**, 3587-3600.

Astley, H. C. and Roberts, T. J. (2012). Evidence for a vertebrate catapult: elastic energy storage in the plantaris tendon during frog jumping. *Biol. Lett.* **8**, 386-389.

Astley, H. C., Abbott, E. M., Azizi, E., Marsh, R. L. and Roberts, T. J. (2013). Chasing maximal performance: a cautionary tale from the celebrated jumping frogs of Calaveras County. *J. Exp. Biol.* **216**, 3947-3953.

Azizi, E. and Brainerd, E. L. (2007). Architectural gear ratio and muscle fiber strain homogeneity in segmented musculature. *J. Exp. Zool. A Ecol. Genet. Physiol.* **307A**, 145-155.

Ballintijn, C. (1969). Functional anatomy and movement co-ordination of the respiratory pump of the carp (*Cyprinus carpio* L.). *J. Exp. Biol.* **50**, 547-567.

Brainerd, E. L., Baier, D. B., Gatesy, S. M., Hedrick, T. L., Metzger, K. A., Gilbert, S. L. and Crisco, J. J. (2010). X-ray reconstruction of moving morphology (XROMM): precision, accuracy and applications in comparative biomechanics research. *J. Exp. Zool.* **313A**, 262-279.

Camp, A. L. and Brainerd, E. L. (2014). Role of axial muscles in powering mouth expansion during suction feeding in largemouth bass (*Micropterus salmoides*). *J. Exp. Biol.* **217**, 1333-1345.

Camp, A. L. and Brainerd, E. L. (2015). Reevaluating musculoskeletal linkages in suction-feeding fishes with X-Ray Reconstruction of Moving Morphology (XROMM). *Integr. Comp. Biol.* **55**, 36-47.

Camp, A. L., Roberts, T. J. and Brainerd, E. L. (2015). Swimming muscles power suction feeding in largemouth bass. *Proc. Natl. Acad. Sci. USA* **112**, 8690-8695.

Camp, A. L., Astley, H. C., Horner, A. M., Roberts, T. J. and Brainerd, E. L. (2016). Fluoromicrometry: a method for measuring muscle length dynamics with biplanar videofluoroscopy. *J. Exp. Zool. A* **325A**, 399-408.

Carroll, A. M. and Wainwright, P. C. (2006). Muscle function and power output during suction feeding in largemouth bass, *Micropterus salmoides*. *Comp. Biochem. Physiol. A Mol. Integr. Physiol.* **143**, 389-399.

Carroll, A. M. and Wainwright, P. C. (2009). Energetic limitations on suction feeding performance in centrarchid fishes. *J. Exp. Biol.* **212**, 3241-3251.

Carroll, A. M., Ambrose, A. M., Anderson, T. A. and Coughlin, D. J. (2009). Feeding muscles scale differently from swimming muscles in sunfish (Centrarchidae). *Biol. Lett.* **5**, 274-277.
Coughlin, D. J. and Carroll, A. M. (2006). In vitro estimates of power output by epaxial muscle during feeding in largemouth bass. *Comp. Biochem. Physiol. A Mol. Integr. Physiol.* **145**, 533-539.
Curtin, N. A., Woledge, R. C. and Aerts, P. (2005). Muscle directly meets the vast power demands in agile lizards. *Proc. R. Soc. B Biol. Sci.* **272**, 581-584.
Day, S. W., Higham, T. E., Holzman, R. and Van Wassenbergh, S. (2015). Morphology, kinematics, and dynamics: the mechanics of suction feeding in fishes. *Integr. Comp. Biol.* **55**, 21-35.
Elshoud-Oldenhave, M. J. W. (1979). Prey capture in the Pike-Perch, *Stizostedion lucioperca* (Teleostei, Percidae): a structural and functional analysis. *Zoomorphologie* **93**, 1-32.
Frith, H. and Blake, R. (1995). The mechanical power output and hydromechanical efficiency of northern pike (Esox lucius) fast-starts. *J. Exp. Biol.* **198**, 1863.
Gatesy, S. M., Baier, D. B., Jenkins, F. A. and Dial, K. P. (2010). Scientific rotoscoping: a morphology-based method of 3-D motion analysis and visualization. *J. Exp. Zool.* **313**, 244-261.
Gemballa, S. and Vogel, F. (2002). Spatial arrangement of white muscle fibers and myoseptal tendons in fishes. *Comp. Biochem. Physiol. A Mol. Integr. Physiol.* **133**, 1013-1037.
Grubich, J. R. (2001). Prey capture in actinopterygian fishes: a review of suction feeding motor patterns with new evidence from an elopomorph fish, *Megalops atlanticus*. *Am. Zool.* **41**, 1258-1265.
Higham, T. E., Day, S. W. and Wainwright, P. C. (2006a). The pressures of suction feeding: the relation between buccal pressure and induced fluid speed in centrarchid fishes. *J. Exp. Biol.* **209**, 3281-3287.
Higham, T. E., Day, S. W. and Wainwright, P. C. (2006b). Multidimensional analysis of suction feeding performance in fishes: fluid speed, acceleration, strike accuracy and the ingested volume of water. *J. Exp. Biol.* **209**, 2713-2725.
Knörlein, B. J., Baier, D. B., Gatesy, S. M., Laurence-Chasen, J. D. and Brainerd, E. L. (2016). Validation of XMALab software for marker-based XROMM. *J. Exp. Biol.* **219**, 3701-3711.
Lauder, G. (1980). The suction feeding mechanism in sunfishes (Lepomis) - an experimental analysis. *J. Exp. Biol.* **88**, 49-72.
Lauder, G. V. (1985). Aquatic feeding in lower vertebrates. In *Functional Vertebrate Morphology* (ed. M. Hildebrand et al.), pp. 185-229. Cambridge, MA: Harvard Univ Press.
Lauder, G. and Lanyon, L. (1980). Functional anatomy of feeding in the bluegill sunfish, *Lepomis macrochirus*: in vivo measurement of bone strain. *J. Exp. Biol.* 84, 33-55.
Lauder, G. V., Wainwright, P. C. and Findeis, E. (1986). Physiological mechanisms of aquatic prey capture in sunfishes: functional determinants of buccal pressure changes. *Comp. Biochem. Physiol. A Physiol.* **84**, 729-734.
Liem, K. F. (1967). Functional morphology of the head of the anabantoid teleost fish *Helostoma temmincki*. *J. Morphol.* **121**, 135-157.
Liem, K. F. (1978). Modulatory multiplicity in the functional repertoire of the feeding mechanism in cichlid fishes. I. Piscivores. *J. Morphol.* **158**, 323-360.
Liem, K. F. (1980). Aquistion of energy by teleosts: adaptive mechanisms and evolutionary patterns. In *Environmental Physiology of Fishes* (ed. M. A. Ali), pp. 299-334. New York, NY: Plenum Publishing Corporation.
Marsh, R. L., Olson, J. M. and Guzik, S. K. (1992). Mechanical performance of scallop adductor muscle during swimming. *Nature* **357**, 411-413.
Mendez, J. and Keys, A. (1960). Density and composition of mammalian muscle. *Metabolism* **9**, 184-188.
Muller, M., Osse, J. W. M. and Verhagen, J. H. G. (1982). A quantitative hydrodynamical model of suction feeding in fish. *J. Theor. Biol.* **95**, 49-79.
Near, T. J., Bolnick, D. I. and Wainwright, P. C. (2004). Investigating phylogenetic relationships of sunfishes and black basses (Actinopterygii: Centrarchidae) using DNA sequences from mitochondrial and nuclear genes. *Mol. Phylogen. Evol.* **32**, 344-357.
Norton, S. F. and Brainerd, E. L. (1993). Convergence in the feeding mechanics of ecomorphologically similar species in the Centrarchidae and Cichlidae. *J. Exp. Biol.* **176**, 11-29.
Peplowski, M. M. and Marsh, R. L. (1997). Work and power output in the hindlimb muscles of cuban tree frogs *Osteopilus septentrionalis* during jumping. *J. Exp. Biol.* **200**, 2861-2870.
Rome, L. C. and Sosnicki, A. A. (1991). Myofilament overlap in swimming carp. II. Sarcomere length changes during swimming. *Am. J. Physiol.* **260**, C289-C296.
Rome, L. C., Funke, R. P., Alexander, R. M. N., Lutz, G., Aldridge, H., Scott, F. and Freadman, M. (1988). Why animals have different muscle fibre types. *Nature* **335**, 824-827.
Shadwick, R. E., Steffensen, J. F., Katz, S. L. and Knower, T. (1998). Muscle dynamics in fish during steady swimming. *Am. Zool.* **38**, 755-770.
Smith, A. J., Nelson-Maney, N., Parsons, K. J., James Cooper, W. and Craig Albertson, R. (2015). Body shape evolution in sunfishes: divergent paths to accelerated rates of speciation in the Centrarchidae. *Evol. Biol.* **42**, 283-295.
Van Wassenbergh, S. (2015). A solution strategy to include the opening of the Opercular slits in moving-mesh CFD models of suction feeding. *Integr. Comp. Biol.* **55**, 62-73.
Van Wassenbergh, S., Herrel, A., Adriaens, D. and Aerts, P. (2005). A test of mouth-opening and hyoid-depression mechanisms during prey capture in a catfish using high-speed cineradiography. *J. Exp. Biol.* **208**, 4627-4639.
Van Wassenbergh, S., Herrel, A., Adriaens, D. and Aerts, P. (2007). Interspecific variation in sternohyoideus muscle morphology in clariid catfishes: functional implications for suction feeding. *J. Morphol.* **268**, 232-242.
Van Wassenbergh, S., Strother, J. A., Flammang, B. E., Ferry-Graham, L. A. and Aerts, P. (2008). Extremely fast prey capture in pipefish is powered by elastic recoil. *J. R Soc. Interface* **5**, 285-296.
Van Wassenbergh, S., Lieben, T., Herrel, A., Huysentruyt, F., Geerinckx, T., Adriaens, D. and Aerts, P. (2009a). Kinematics of benthic suction feeding in Callichthyidae and Mochokidae, with functional implications for the evolution of food scraping in catfishes. *J. Exp. Biol.* **212**, 116-125.
Van Wassenbergh, S., Roos, G., Genbrugge, A., Leysen, H., Aerts, P., Adriaens, D. and Herrel, A. (2009b). Suction is kid's play: extremely fast suction in newborn seahorses. *Biol. Lett.* **5**, 200-203.
Van Wassenbergh, S., Dries, B. and Herrel, A. (2014). New insights into muscle function during pivot feeding in seahorses. *PLoS ONE* **9**, e109068.
Van Wassenbergh, S., Day, S. W., Hernández, L. P., Higham, T. E. and Skorczewski, T. (2015). Suction power output and the inertial cost of rotating the neurocranium to generate suction in fish. *J. Theor. Biol.* **372**, 159-167.
Wainwright, P. C., McGee, M. D., Longo, S. J. and Hernandez, L. P. (2015). Origins, innovations, and diversification of suction feeding in vertebrates. *Integr. Comp. Biol.* **55**, 134-145.
Werner, E. E. (1977). Species packing and niche complementarity in three sunfishes. *Am. Nat.* **111**, 553-578.
Westneat, M. W. (2006). Skull biomechanics and suction feeding in fishes. In *Fish Physiology* (ed. R. E. Shadwick and G. Lauder), pp. 29-75. San Diego, CA: Academic Press.

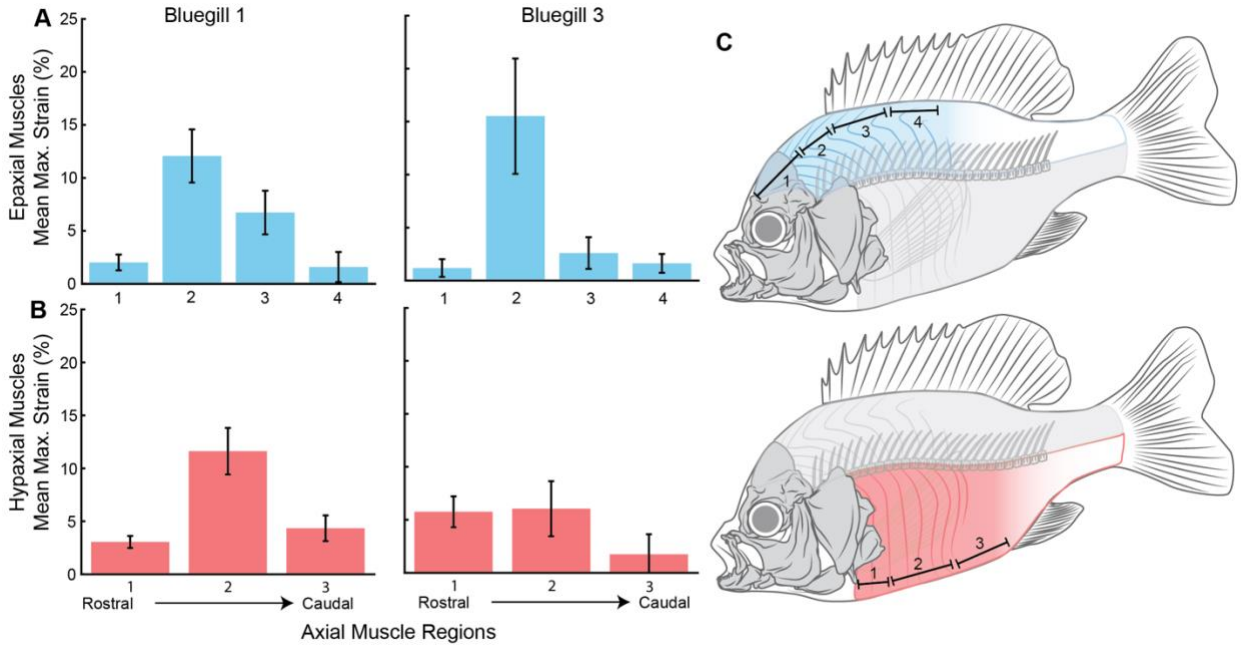

Supplementary Figure S1: Regional muscle strain across the axial muscles. Mean maximum muscle strain in 4 regions of the epaxials (**A**) and 3 regions of the hypaxials (**B**) in each fish. Muscle strains were calculated relative the mean initial length of the muscle region, with positive values indicating shortening. Means are shown with standard error bars (N = 6 strikes for Bluegill 1, N = 5 strikes for Bluegill 3). (**C**) The approximate location of each muscle region.

Supplementary Table S1. Mean (s.e.m) timing and magnitude of peak bone motion, as measured relative to the body plane with JCSs during suction feeding (rot, rotation; trans, translation).

Bone	Variable	Bluegill 1 (N = 6)	Bluegill 3 (N = 5)
Neurocranium	X-rot (°)	1.6 (0.6)	1.2 (0.4)
	Y-rot (°)	-1.8 (1.1)	-3.2 (1.6)
	Z-rot (°)	11.9 (1.6)	13.7 (2.1)
	X-trans (mm)	-0.3 (0.05)	-0.2 (0.1)
	Y-trans (mm)	-0.2 (0.04)	-0.4 (0.2)
	Z-trans (mm)	-1.2 (0.3)	-0.7 (0.3)
	Time[a] of peak Z-rot (ms)	10.0 (3.7)	8.7 (1.8)
Cleithrum	X-rot (°)	2.1 (0.5)	2.4 (0.6)
	Y-rot (°)	-4.2 (1.0)	-4.5 (0.6)
	Z-rot (°)	-7.1 (0.7)	-4.6 (1.0)
	X-trans (mm)	-0.9 (0.1)	-0.7 (0.3)
	Y-trans (mm)	-0.3 (0.04)	-0.2 (0.1)
	Z-trans (mm)	-1.0 (0.2)	-0.5 (0.1)
	Time[a] of peak Z-rot (ms)	11.3 (1.9)	7.7 (1.9)
Urohyal	X-trans (mm)	-3.8 (0.5)	-1.7 (0.6)
	Y-trans (mm)	-7.9 (0.2)	-5.3 (0.5)
	Z-trans (mm)	0.8 (0.5)	2.2 (0.4)
	Time [a] of peak X-trans (ms)	11.7 (1.3)	7.6 (2.0)
	Time[a] of peak Y-trans (ms)	14.0 (2.8)	14.8 (6.5)

[a]Time relative to the time of peak gape

Supplementary Movies

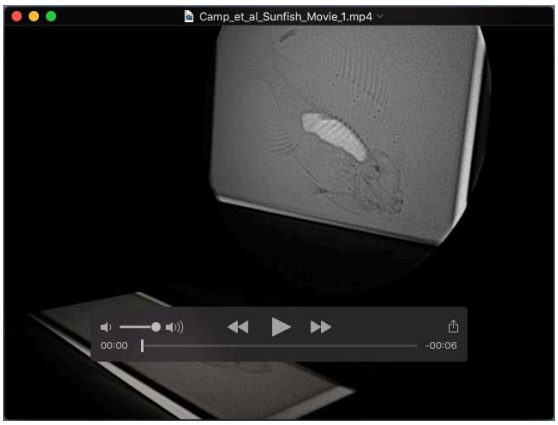

Movie 1: Animation of 3D bone models from X-ray Reconstruction of Moving Morphology (XROMM) during a sample bluegill sunfish suction feeding strike. The animated bones are the neurocranium and cranial bones from the left side of the head, with their medial sides shown here in oblique right lateral view. Also shown are the biplanar X-ray videos from which these motions were reconstructed. The X-ray videos were filmed at 500 Hz, but have been slowed down about 30 times in this movie.

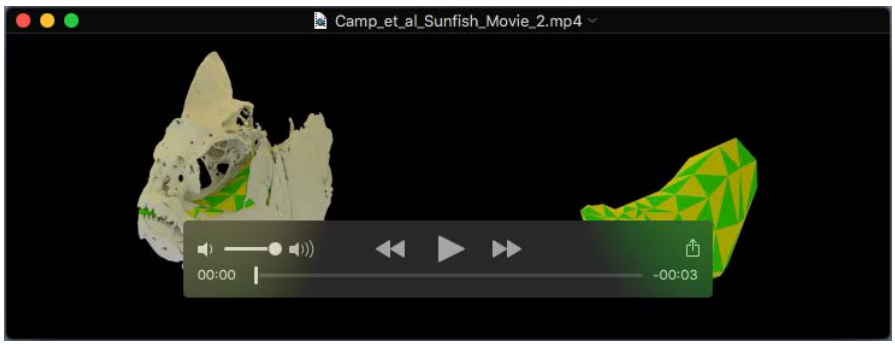

Movie 2: Animation of skeletal kinematics and buccal cavity volume during a sample bluegill sunfish suction feeding strike (antero-lateral view). Buccal volume was measured with a dynamic digital endocast (green and yellow polygon), which is shown with the animated bone models (left) and by itself (right). The motion of both the endocast and the bones are viewed relative to the body plane, i.e., the motion of the fish's body. The animation was created from X-ray videos filmed at 500 Hz, but it has been slowed down about 30 times in this movie.